In Silico Design of Saccharomyces cerevisiae Strains for Improved Production of Chondroitin

Márcia R. Couto , Joana L. Rodrigues * , Oscar Dias , Lígia R Rodrigues

Posted Date: 20 December 2023

doi: 10.20944/preprints202312.1479.v1

Keywords: chondroitin; Saccharomyces cerevisiae; metabolic models; metabolic engineering

Article

In Silico Design of *Saccharomyces cerevisiae* Strains for Improved Production of Chondroitin

Márcia R. Couto [1], Joana L. Rodrigues [1,2,*], Oscar Dias [1,2] and Lígia R. Rodrigues[1,2]

[1] Centre of Biological Engineering, University of Minho, Braga 4710-057, Portugal; marcia.couto@ceb.uminho.pt (M.R.C); odias@ceb.uminho.pt (O.D); lrmr@deb.uminho.pt (L.R.R)
[2] LABBELS – Associate Laboratory, Braga, Guimarães, Portugal
* Correspondence: joanarodrigues@ceb.uminho.pt; Tel.: +351-253604423

Abstract: Chondroitin sulfate is a glycosaminoglycan that has gained widespread use in nutraceuticals and pharmaceuticals, mainly for treating osteoarthritis. Traditionally, it has been extracted from animal cartilage but recently, biotechnological processes have emerged as a commercial alternative to avoid the risk of viral or prion contamination and offer a vegan-friendly source. Typically, these methods involve producing the chondroitin backbone using pathogenic bacteria and then modifying it enzymatically through the action of sulfotransferases. Despite the challenges of expressing active sulfotransferases in bacteria, the use of eukaryotic microorganisms is still limited to a few works using *Pichia pastoris*. To create a safer and efficient biotechnological platform, we have constructed a biosynthetic pathway for chondroitin production in *S. cerevisiae*. Furthermore, as genome-scale models are valuable tools for identifying novel targets for metabolic engineering, a stoichiometric model of chondroitin-producing *S. cerevisiae* has been developed and used in optimization algorithms. Our research has yielded several novel targets, such as uridine diphosphate(UDP)-*N*-acetylglucosamine pyrophosphorylase (*QRI1*), glucosamine-6-phosphate acetyltransferase (*GNA1*) or *N*-acetylglucosamine-phosphate mutase *(PCM1*) overexpression that might enhance chondroitin production, which will guide future experimental research to develop more efficient host organisms for the biotechnological production process.

Keywords: chondroitin; *Saccharomyces cerevisiae*; metabolic models; metabolic engineering

1. Introduction

Chondroitin sulfate is a glycosaminoglycan that naturally occurs in animals, in different concentrations, and in different sulfation patterns, percentage and structure ratios, according to the tissue where it is present [1]. Unsulfated or fructosylated forms of this compound also exist in some pathogenic bacteria as a capsular constituent [2]. Chondroitin sulfate has been mainly used in nutraceuticals, pharmaceuticals and veterinary supplements for osteoarthritis treatment and joint protection, but also in ophthalmological solutions and devices. Its biological activity varies according to its sulfonation pattern, therefore making it versatile and useful in a wide range of other potential applications [1]. The biotechnological production of chondroitin is generally based on cultivating the pathogenic bacteria *Escherichia coli* O5:K4:H4, which naturally produces a fructosylated form of chondroitin [3]. Many efforts have been made to engineer chondroitin production using safer microorganisms [4–7], however the yields do not meet the growing demand. Furthermore, eukaryotic microorganisms remain relatively unexplored, with a single work using *Pichia pastoris* for chondroitin production [8]. Nevertheless, eukaryotic microorganisms are particularly interesting for chondroitin production because of their ability to perform post-translational modifications, unlike prokaryotic organisms such as *E. coli*. In fact, glycosylation and correct folding are required for animal sulfotransferases to become active and perform the sulfonation of the chondroitin backbone [9], which makes the correct expression of these proteins challenging, especially in prokaryotic hosts [10]. *S. cerevisiae* has been one of the most widely used microbes for industrial biotechnological production

 doi:10.20944/preprints202312.1479.v1

of several compounds. Its broad use as host in metabolic engineer is related to its rapid and robust growth, its ease of genetic manipulation for recombinant protein expression, and its ability to perform post-translational modifications, including glycosylation, and to properly fold recombinant proteins [11–13]. Therefore, it can be an interesting host to be used in the production of chondroitin.

Genome-scale metabolic models (GEMs) are powerful resources that consist in the representation of the entire metabolic network of a biological system, including the enzymes, metabolites, reactions, genes, and their associations, containing information on stoichiometry, compartmentalization and biomass composition [14]. The use of these models to evaluate the organism biological capabilities requires the representation of the biochemical conversions following a stoichiometric matrix representation containing the stoichiometric coefficients for each metabolite in each reaction, where reactions are the columns and the metabolites the rows [14,15]. Constraint-based modelling assumes that cells operate in a steady-state, meaning that the metabolites may not be accumulated, and by applying flux constrains through upper and lower bounds, this matrix is transformed into a system of linear equations which can be used to calculate the flux of each reaction [14,15]. As this represents an undetermined system, a biological relevant reaction, usually biomass production, is used as the objective function to formulate a linear problem that can be solved using mathematical programming [14]. Manipulating the reaction bounds allows to simulate environmental conditions or genetic modifications such as knockouts [16]. Appling evolutionary algorithms is a common strategy in strain design for identifying targets for metabolic engineering. Additionally, other information can be integrated with GEMs such as regulatory, kinetics and omics data to improve the predictive power of these models in specific conditions [17].

As GEMs provide a systems biology framework for phenotype simulation, they have wide applications in metabolism studying, identification of novel targets for metabolic engineering, diseases understanding and drug target identification [14,18–22]. In particular, the industrial applications of GEMs are the most reported as they have been used for enhancing the biotechnological production of several compounds, either endogenous or heterologous, such as dicarboxylic acids [23–29], alcohols [30–32], amino acids [33–35], polymers [36–39], antibiotics [40,41] and polyphenols [42–44].

This study explores the potential of chondroitin sulfate production in *S. cerevisiae* using synthetic biology and metabolic engineering strategies. Furthermore, using a budding yeast GEM, *in silico* flux analysis was employed, as well as evolutionary algorithms, to identify novel targets for improving chondroitin titers.

2. Materials and Methods

2.1. Model construction

The consensus GEM of *Saccharomyces cerevisiae* yeast-GEM [45], version 8.4.2 (https://github.com/SysBioChalmers/yeast-GEM), composed by 4058 reactions, 2742 metabolites and 1150 genes, was used as template. From this, a new model containing the heterologous pathway for chondroitin production was constructed by including the reactions UGD (uridine diphosphate(UDP)-glucose 6-dehydrogenase), UAE (UDP-*N*-acetylglucosamine 4-epimerase), CHSY (chondroitin synthase/polymerase) and EX_chond (chondroitin drain reaction). The metabolites UDP-glucose (S_1543) and UDP-acetylglucosamine (S_1544) were already available in the template model. UDP-glucuronic acid (M_udpglcur), UDP-acetylgalactosamine (M_udpacgal) and chondroitin (M_chond) were included. The genes for the reactions UGD, UAE and CHSY were also included in the model. After preliminary tests, the biomass equation was adjusted to include 1% chitin in biomass composition. The final model, labelled yeast-GEM_c, includes 4062 reactions, 2745 metabolites and 1153 genes.

2.2. Conditions for in silico simulations and optimization

The OptFlux software [46] (version 3.3.5) was used to simulate the phenotype of *S. cerevisiae* engineered with chondroitin production pathway and further mutants, using parsimonious Flux

 doi:10.20944/preprints202312.1479.v1

Balance Analysis (pFBA) as simulation method [47]. The glucose uptake was set to 10 mmol/gDW/h and oxygen was unrestricted (1000 mmol/gDW/h). The identification of gene deletion and over / under expression targets to optimize chondroitin production was performed by running optimization algorithms. Strength Pareto Evolutionary Algorithm 2 (SPEA2) [48] was used as optimization strategy where the Biomass-Product Coupled Yield (BPCY) was set as the objective, and pFBA as the simulation method. pFBA used biomass reaction (r_2111) as the objective function to maximize. A maximum of 10 modifications were allowed. The maximum for evaluation functions was set to 50,000. CPLEX Optimization Studio version 12.9.0 (IBM) was used as Linear Programming solver.

The identification of chondroitin optimization targets was also performed with MEWpy [49] under the same environmental conditions as before, using the Evolutionary Algorithm Non-Dominated Sorting Genetic Algorithm II [50] as optimization strategy and pFBA as the simulation method. The evolutionary algorithm employed two objective functions, BPCY and Weighted Yield (WYIELD, weighed sum of the minimum and maximum product fluxes). pFBA used the biomass reaction as the objective function to maximize. A maximum of 10 or 3 modifications were allowed.

Flux variability analysis (FVA) of chondroitin production [51] was performed to assess the robustness of the optimization results.

2.3. Strains and plasmids

The strains and plasmids used in this study are listed in Table 1. *E. coli* NZY5α (NZYTech, Lisbon, Portugal) competent cells were used for cloning procedures, vector propagation and storage. *E. coli* was cultured at 37°C and 200 rpm in lysogeny broth (LB) (10 g/L tryptone, 5 g/L yeast extract, 10 g/L NaCl; NZYTech) or on LB agar plates (20 g/L agar, JMGS, Odivelas, Portugal). Ampicillin (NZYTech) at a final concentration of 100 μg/mL was supplemented when necessary.

Table 1. Strains and plasmids used in this study.

Strains	**Relevant genotype**	**Source**
Escherichia coli NZY5α	*fhuA2* Δ(*argF-lacZ*)U169 *phoA glnV44*Φ80 Δ(*lacZ*)M15 *gyrA96 recA1 relA1 endA1 thi-1 hsdR17*	NZYTech (MB00401)
Saccharomyces cerevisiae CEN.PK2-1C	*MATa ura3-52 his3Δ1 leu2-3,112 trp1-289 MAL2-8^{c} SUC2*	Euroscarf 30000A [52]
S. cerevisiae BY4741	*MATa his3Δ1 leu2Δ0 met15Δ0 ura3Δ0*	Euroscarf Y00000 [53]
Plasmids	**Description**	**Source**
pSP-GM1	pUC *ori*, Amp^{R}, 2 μ *ori*, *URA3* P_{TEF1} P_{PGK1}	Addgene #64739 [54]
pBEVY-L	pUC *ori*, Amp^{R}, 2 μ *ori*, *LEU2* P_{GPD} P_{ADH1}	ATCC 51226
pUC57_Giuae	pMB1 *ori*, Amp^{R}; pUC57 carrying *Giardia intestinalis* uridine diphosphate-glucosamine-4-epimerase gene (*GiUAE*) codon-optimized for *S. cerevisiae*	NZYTech
pUC57_Btchsy1	pMB1 *ori*, Amp^{R}; pUC57 carrying *Bos taurus* chondroitin synthase 1 gene (*BtCHSY*) codon-optimized for *S. cerevisiae*	NZYTech
pETM6_kfoCA	pETM6 carrying chondroitin synthase, *kfoC*, and, uridine diphosphate-glucosamine-4-epimerase, *kfoA*, genes from *E. coli* O5:K4:H4	[5]
pSP-GM1_Zmugd	pSP-GM1 carrying *Zymomonas mobilis* uridine diphosphate glucose 6-dehydrogenase gene (*Zmugd*)	[55]
pSP-GM1_Giuae_Zmugd	pSP-GM1 carrying *GiUAE* and *Zmugd*	This study
pBEVY_Btchsy	pBEVY-L carrying *BtCHSY*	This study
pSP-GM1_kfoA_Zmugd	pSP-GM1 carrying *kfoA* and *Zmugd*	This study

 doi:10.20944/preprints202312.1479.v1

Strains	Relevant genotype	Source
pBEVY_kfoC	pBEVY-L carrying *kfoC*	This study

S. cerevisiae CEN.PK2-1C and *S. cerevisiae* BY4741 strains were obtained from Euroscarf (Oberursel, Germany). The plasmids pSP-GM1 (PGK1 promoter and TEF promoter; Addgene, Watertown, MA, USA) and pBEVY-L (GPD promoter; ATCC, Manassas, USA) were used as shuttle vectors. Wild-type yeast strains were cultivated at 30°C and 200 rpm in yeast extract peptone dextrose (YPD) media, composed by 20 g/L bacteriological peptone (HiMedia, Mumbai, India), 10 g/L yeast extract (Panreac AppliChem, Darmstadt, Germany), 20 g/L glucose (Acros Organics, New Jersey, USA), or in agar plates with the same composition.

The engineered yeast strains were grown in synthetic defined minimal media composed by 6.7 g L^{-1} of yeast nitrogen base (YNB) with ammonium sulfate without amino acids (Sigma Aldrich, Steinheim, Germany), supplemented with 20 g/L glucose and the required amino acids to compensate for auxotrophies, namely tryptophan or methionine (Panreac AppliChem), depending on the strain, and histidine (Panreac AppliChem) at final concentrations of 100 mg/L.

2.4. Biosynthetic pathway construction

Table S1 compiles the primers used for cloning procedures. Two different biosynthetic pathways have been constructed and introduced in *S. cerevisiae* CEN.PK2-1C and *S. cerevisiae* BY4741 strains. Each pathway contained three genes for the expression of UGD, UAE and CHSY, which are absent in yeast metabolism. UAE gene from *Giardia intestinalis* (GenBank accession number AY187036.1, *GiUAE*) and CHSY gene from *Bos taurus* (GenBank accession number AF440749.1, *BtCHSY*) were codon-optimized for *S. cerevisiae* and synthesized by NZYTech (sequences can be seen in Table S2). Afterwards, *GiUAE* and *BtCHSY* were amplified from pUC57_Giuae and pUC57_Btchsy, respectively, using Gi_uae_Fw1 and Gi_uae_Rv1 or Bt_chsy1_Fw and Bt_chsy1_Rv as primers. After amplification, genes were first independently cloned in pSP-GM1 under PGK1 promoter. For further assembly of the entire chondroitin pathway, the *GiUAE* was cloned in pSP-GM1 under the TEF promoter regulation, using the primers Giuae_tefp_Fw and Giuae_tefp_Rv for gene amplification. Then, *Zmugd*, amplified from pSP-GM1_Zmugd [55] with primers Zm_psp_Fw and Zm_psp_Rv, was cloned in pSP-GM1_Giuae_tef, resulting in pSP-GM1_Giuae_Zmugd (*Zmugd* was cloned second as the restriction enzymes used to clone *GiUAE* cut *Zmugd*, that is not codon-optimized). The *BtCHSY* was amplified from pSP-GM1_Btchsy, using the primers Btchsy_pBEVY_Fw and Btchsy_pBEVY_Rv, and cloned in pBEVY-L generating pBEVY_Btchsy. The second pathway was composed by chondroitin-producing genes *kfoA* and *kfoC* (encoding UAE and CHSY, respectively) from *E. coli* K4 (serotype O5:K4(L):H4). *KfoA* and *kfoC* were amplified from pETM6_kfoCA [5], which was kindly provided by Dr. Mattheos Koffas (Rensselaer Polytechnic Institute, Troy, NY). For that purpose, the primer pairs kfoA_psp_Fw/kfoA_psp_Rv and kfoC_pBEVY_Fw/kfoC_pBEVY_Rv were used, respectively. Then, *kfoA* was cloned into pSP-GM1_Zmugd [55] while *kfoC* was cloned in pBEVY-L, resulting in pSP-GM1_kfoA_Zmugd and pBEVY_kfoC, respectively.

All gene amplifications were performed through PCR (polymerase chain reaction) using phusion High Fidelity DNA Polymerase (Thermo Fisher Scientific, Wilmington, United States). The plasmids were extracted with Plasmid Miniprep Kit (Macherey-Nagel, Düren, Germany). PCR products from amplification were excised and purified from agarose gels using NucleoSpin® Gel and PCR Clean-up Kit (Macherey-Nagel). Quantification of plasmid DNA and PCR products was further achieved using NanoDrop One instrument (Thermo Fisher Scientific). Then, digestion was performed by incubating specific restriction endonucleases (Thermo Fisher Scientific) for 1 h at 37°C. The resulting digested DNA fragments were purified using NucleoSpin® Gel and PCR Clean-up Kit and used for ligations with T4 DNA ligase (Thermo Fisher Scientific) for 1 h at room temperature. The resulting mixture was transformed into *E. coli* NZY5α competent cells (NZYTech) by heat shock. Transformants were then recovered by adding super optimal broth with catabolite repression (SOC; NZYTech) and incubating the mixture for 1 h at 37°C. Cells were then platted on agar plates containing selective medium. Finally, all construction sequences were verified by colony PCR using

 doi:10.20944/preprints202312.1479.v1

Dream Taq polymerase (Thermo Fisher Scientific), digestion, and further confirmation by sequencing (GATC Biotech, Konstanz, Germany). After sequence confirmation, transformations of the constructed plasmids into *S. cerevisiae* were performed by lithium acetate/single-stranded carrier DNA/polyethylene glycol method [56]. Lithium acetate, salmon sperm DNA and polyethylene glycol (PEG-3350) were obtained from Sigma-Aldrich. Selection of yeast transformants was performed in synthetic defined minimal media with the required amino acids.

2.5. Flask fermentation conditions

For each assay, a single *S. cerevisiae* colony was picked from the transformation plate and grown for 24 h at 30°C and 200 rpm in 8 mL of the synthetic defined minimal media supplemented with the required amino acids for pre-culture. Afterwards, 50 mL of medium with the same composition in 250 mL flasks were inoculated to an initial optical density at 600 nm (OD_{600nm}) of 0.1. Yeast cells were further cultured at 30°C and 200 rpm for 24 h.

2.6. Analytical methods

In the end of the fermentation, the culture of *S. cerevisiae* cells (~50 mL) was harvested by centrifugation (5,000 × g, 15 min). The supernatants were used to quantify extracellular chondroitin and glucose, while the pellets were further processed to determine intracellular chondroitin.

To obtain the intracellular fraction, cells were lysed. For each 0.1 g of wet cells, 0.2 g of glass beads (425–600 µm, Sigma- Aldrich) were added to the cells pellet, as well as 1 mL of deionized water. Cells were then lysed in FastPrep-24 (MP Biomedicals, Salon, USA) during 5 cycles of 1 min at 6–6.5 m/s interspersed with 1 min cooling on ice. Lysed samples were centrifuged (16,000 × g, 15 min). Afterwards, the lysates (supernatant) were treated with DNaseI (New England Biolabs, MA, USA) for 2 h at 37°C and then with proteinase K (2 mg/mL, NZYTech) for 2 h at 56°C. The mixture was further boiled for 5 min and centrifuged (16,000 x g, 20 min) to remove insoluble material.

To precipitate extracellular and intracellular chondroitin, three volumes of cold ethanol were added to the samples and the mixture was left at 4°C overnight. The resulting precipitate was collected through centrifugation (4,000 x g for 10 min at 4°C) and subsequently air-dried at room temperature overnight. The dried precipitate was resuspended in deionized water followed by removal of the insoluble material by centrifugation (16,000 x g, 20 min). Uronic acid carbazole assay [57] was used to quantify chondroitin by using chondroitin sulfate (Biosynth, Staad, Switzerland) solutions as standards. Standards or samples with 125 µL were mixed with 750 µL sulfuric acid reagent (9.5 g/L sodium tetraborate, Supelco, Bellefonte, USA, dissolved in H_2SO_4 > 95%, Fisher Chemical, Hampton, USA) and boiled for 20 min. Then, 25 µL of carbazole reagent (1.25 g/L carbazole, Supelco, dissolved in absolute ethanol, Fisher Chemical) were added to the boiled samples, followed by an additional 15 min boil and a subsequent 15 min cooling period. The OD_{530nm} was measured using a 96-well plate spectrophotometric reader Synergy HT (BioTek, Winooski, VT, USA).

Yeast cell concentration was calculated by determining the OD_{600nm} in the end of culture, using a calibration with solutions of known biomass concentration.

Glucose samples at the end of fermentation were analyzed using high performance liquid chromatography (HPLC) with a JASCO system and a refractive index (RI) detector (RI-2031), employing an Aminex HPX-87H column from Bio-Rad maintained at 60°C. The mobile phase used was 5 mM H_2SO_4 at a flow rate of 0.5 mL/min.

3. Results

3.1. Bioinformatics tool for identification of gene targets

A model of *S. cerevisiae* metabolism has been modified to include the heterologous reactions, intermediates and genes required for chondroitin production. At that stage, optimizations for improving chondroitin production could not find any solution, either searching for knockout or under- and overexpression targets. One possible hypothesis for this was that biomass growth was not being properly coupled with product formation. We then realized that the original biomass

Preprints (www.preprints.org) | NOT PEER-REVIEWED | Posted: 20 December 2023 doi:10.20944/preprints202312.1479.v1

equation did not predict the inclusion of chitin. Even though *S. cerevisiae* is reported to have a minimal amount of chitin, its presence might still be necessary for essential functions related to cell wall integrity and other processes, as suggested by the finding that simultaneous knockout of all three chitin synthase genes is lethal in yeast [58]. Therefore, based on literature [59–61], the biomass equation was corrected to include 1% chitin, by adjusting the reaction stoichiometry in the model to maintain the stoichiometric coefficients of other compounds while including the necessary stoichiometric coefficient to achieve the desired percentage of chitin (Table 2). As chitin is an important intervenient in pathways related with chondroitin precursors, this adjustment could result in optimization results.

Table 2. Intermediates and their stoichiometric values in growth equation in the model yeast-GEM 8.4.2 before and after including 1% of chitin.

Compound ID code	Compound name	Template model		Corrected model 1% chitin	
		Stoichiometry	Percentage (%)	Stoichiometry	Percentage (%)
s_0001_ce	(1→3)-β-D-glucan [cell envelope]	0.748514964	33.88	0.748514964	33.54
s_0004_ce	(1→6)-β-D-glucan [cell envelope]	0.250091654	11.32	0.250091654	11.21
s_0773_c	glycogen [cytoplasm]	0.361414528	16.36	0.361414528	16.20
s_1107_c	mannan [cytoplasm]	0.710939625	32.18	0.710939625	31.86
s_1520_c	trehalose [cytoplasm]	0.138275712	6.26	0.138275712	6.20
s_0509_c	chitin [cytoplasm]	0	0.00	0.022313288	1.00

In fact, after performing these modifications, the optimization using evolutionary algorithms in OptFlux was able to find multiple solutions. The solutions with best BPCY are shown in Table 3.

Table 3. Optimization of chondroitin production in yeast-GEM_c model using OptFlux. The optimization algorithm for under and overexpression identification was run three times. The predicted phenotype for the unmodified and modified strains (from the resulting solutions with highest biomass-product coupled yield, BPCY) are shown. The growth rate and chondroitin production rate are presented in units of h^{-1} and mmol/g_{DW}/h, respectively. BPCY is calculated by OptFlux by multiplying biomass by product and then dividing by substrate consumed (in all cases being 10 mmol/gDW/h), as predicted by pFBA simulation. Flux variability analysis (FVA) results are shown as minimum and maximum chondroitin obtained through pFBA for fixed biomass.

Solution	BPCY	Genes modified		Predicted phenotype (pFBA)		FVA	
		Under expression	Over expression	Biomass (h^{-1})	Chondroitin flux (mmol/g_{DW}/h)	Minimum chondroitin flux (mmol/g_{DW}/h)	Maximum chondroitin flux (mmol/g_{DW}/h)
-	-	-	-	0.8612	0.0000	-	-
1	0.04375	-	*QRI1*	0.7317	0.5980	0.5980	0.9358
2	0.04375	-	*GNA1*	0.7317	0.5980	0.5980	0.9358
3	0.04375	-	*PCM1*	0.7317	0.5980	0.5980	0.9358

Gene descriptions: *GNA1* - glucosamine-6-phosphate acetyltransferase; *PCM1* - *N*-acetylglucosamine-phosphate mutase; *QRI1* – uridine diphosphate-*N*-acetylglucosamine pyrophosphorylase.

Despite allowing for ten modifications, the solutions pointed to single modifications, namely the overexpression of one of the genes involved in the production of chondroitin precursors, *QRI1*, *GNA1* or *PCM1* (expression values of 32). *GNA1* encodes glucosamine-6-phosphate acetyltransferase, which catalyzes *N*-acetylglucosamine 6-phosphate synthesis, from glucosamine 6-phosphate and acetyl-coenzyme A (acetyl-CoA). *PCM1*, encoding *N*-acetylglucosamine-phosphate mutase, is responsible for converting *N*-acetylglucosamine 6-phostate to *N*--acetylglucosamine 1-phostate. *QRI1*, encoding

Preprints (www.preprints.org) | NOT PEER-REVIEWED | Posted: 20 December 2023 doi:10.20944/preprints202312.1479.v1

UDP-*N*-acetylglucosamine pyrophosphorylase, is responsible for the formation of UDP-*N*-acetylglucosamine. Figure 1 shows a schematic representation of the metabolism of *S. cerevisiae* that is involved in the biosynthetic production of chondroitin and the possible competing pathways.

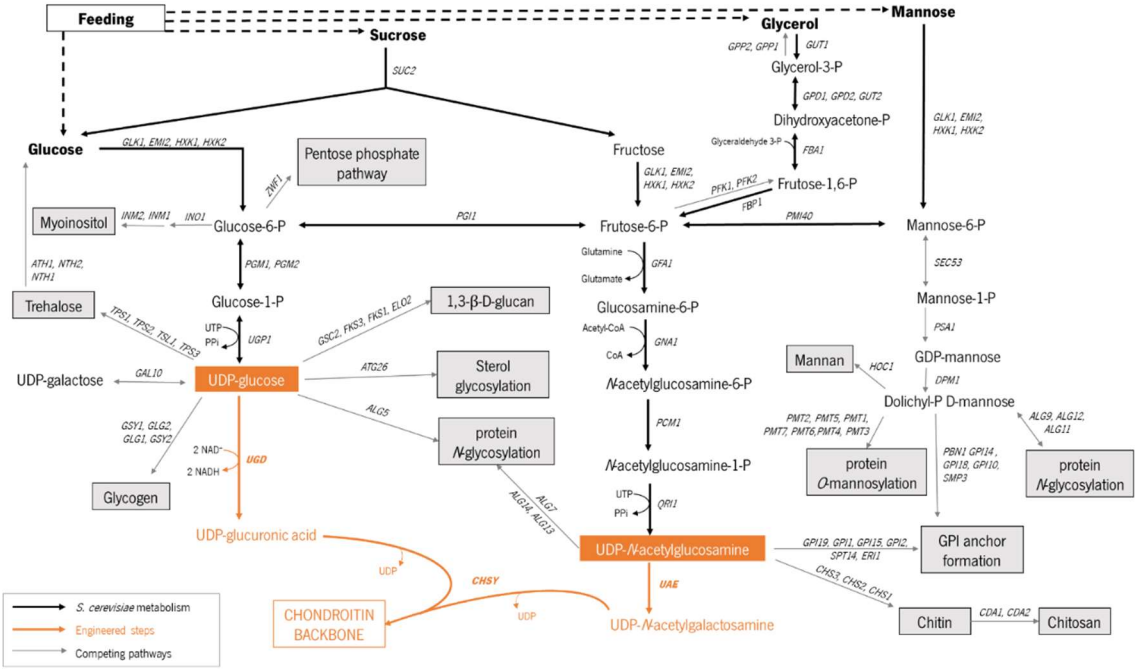

Figure 1. Pathways involved in chondroitin production in engineered *Saccharomyces cerevisiae* cells, and competing pathways that redirect the metabolic flux from chondroitin precursors. **Compound abbreviations:** CoA – coenzyme A; NAD - nicotinamide adenine dinucleotide; PPi – diphosphate; GPI - glycosylphosphatidylinositol; UDP – uridine diphosphate; UTP - uridine triphosphate; **Gene descriptions:** *ALG11* - Alpha-1,2-mannosyltransferase; *ALG12* - Alpha-1,6-mannosyltransferase; *ALG9* – mannosyltransferase; *ALG5* - UDP-glucose:dolichyl-phosphate glucosyltransferase; *ATH1* - acid trehalase; *ATG26* - UDP-glucose:sterol glucosyltransferase; *CDA1*, *CDA2* – chitin deacetylase; *CHS1*, *CHS2*, *CHS3* - chitin synthases; *CHSY* - chondroitin synthase; *DPM1* - dolichol phosphate mannose synthase; *EMI2* - hexokinase; *ERI1* - endoplasmic reticulum-associated Ras Inhibitor; *FBA1* – fructose 1,6-bisphosphate aldolase; *FBP1* - fructose-1,6-bisphosphatase; *FKS1*, *FKS3* - 1,3-β-D-glucan synthase; *GAL10* – UDP-glucose-4-epimerase; *GLG1*, *GLG2* – glycogenin glucosyltransferase; *GLK1* - glucokinase; *GNA1* - glucosamine-6-phosphate *N*-acetyltransferase; *GPD1*, *GPD2* - glycerol-3-phosphate dehydrogenases; *GPI1*, *GPI10*, *GPI14*, *GPI15*, *GPI18*, *GPI19* – GPI anchor proteins; *GPP1*, *GPP2* - glycerol-3-phosphate phosphatases; *GSC2* - 1,3-β-glucan synthase; *GSY1*, *GSY2* - glycogen synthases; *GUT1* - glycerol kinase; *GUT2* - glycerol-3-phosphate dehydrogenase; *HXK1*, *HXK2* - hexokinases; *INO1* - inositol-3-phosphate synthase; *INM1*, *INM2* - inositol monophosphatases; *NTH1*, *NTH2* - neutral trehalases; *PBN1* - glycosylphosphatidylinositol-mannosyltransferase I; *PCM1* - *N*-acetylglucosamine-phosphate mutase; *PFK1*, *PFK2* - phosphofructokinase; *PGI1* - phosphoglucose isomerase; *PMT1*, *PMT2*, *PMT3*, *PMT4*, *PMT5*, *PMT6*, *PMT7* - protein *O*-mannosyltransferases; *PSA1* - guanosine diphosphate(GDP)-mannose pyrophosphorylase; *QRI1* - UDP-*N*-acetylglucosamine pyrophosphorylase; *SEC53* - Phosphomannomutase; *SMP3* - alpha 1,2-mannosyltransferase; *SPT14* - UDP-glycosyltransferase; *SUC2* – invertase; *TPS1* - trehalose-6-phosphate synthase; *TPS2* - trehalose-phosphatase; *TPS3* - trehalose-6-phosphatase; *UAE* - UDP-*N*-acetylglucosamine 4'-epimerase; *UGD* - UDP-glucose 6-dehydrogenase; *ZWF1* - glucose-6-phosphate dehydrogenase.

The overexpression of genes associated with the synthesis of precursors, namely UDP-glucose and UDP-*N*-acetylglucosamine, is a common strategy for improving the production of chondroitin and other glycosaminoglycans [3,7,62–64]. Interestingly, all the optimization results herein obtained indicated genes that lead to UDP-*N*-acetylglucosamine production, suggesting this intermediate as the limiting precursor in *S. cerevisiae*.

Preprints (www.preprints.org) | NOT PEER-REVIEWED | Posted: 20 December 2023 doi:10.20944/preprints202312.1479.v1

Regarding FBA analysis, the difference between the predicted minimum and maximum chondroitin production shows that mutants are moderately robust.

In MEWpy, the optimization using evolutionary algorithms resulted in 75 solutions that included modifications in 53 different genes. The frequency and expression values of genes resulting from optimization are shown in Figure 2.

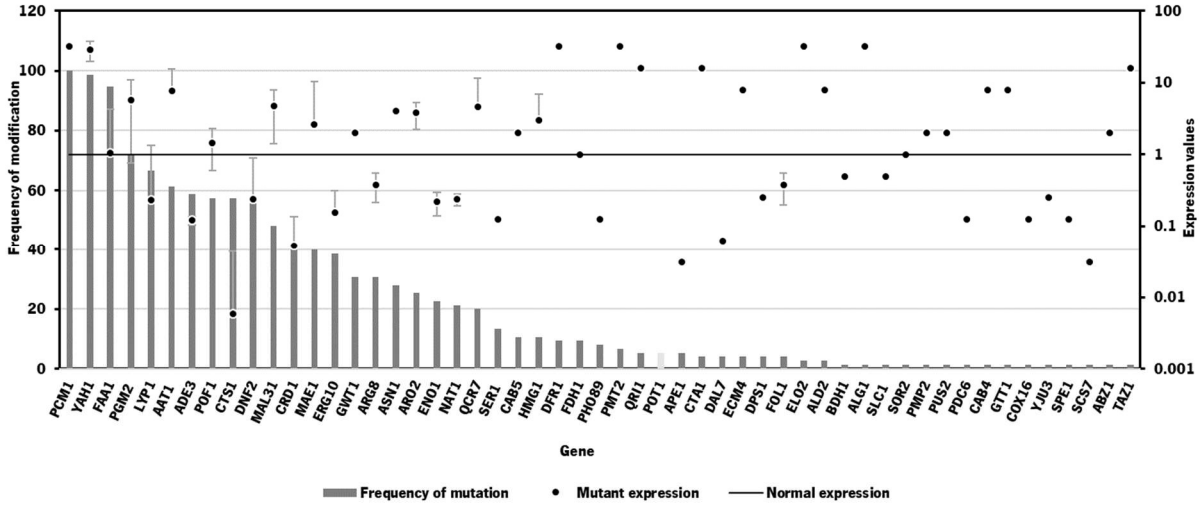

Figure 2. Frequency and expression values of genes in the solutions from optimization of *Saccharomyces cerevisiae* model for chondroitin production using MEWpy tool, limiting number of modifications to 10. The mutant expression (in dots) represents the average expression value. Mutant expressions higher than 1 represent overexpression while values of expression lower than 1 represent underexpression. Deletion is represented using a light grey bar.

All solutions presented one common modification, namely the overexpression of *PCM1*, a modification already identified by the OptFlux approach, which confirms it as a valuable strategy for improving chondroitin titers in engineered yeast cells. *QRI1* overexpression was also identified in the MEWpy approach, but only in four of the solutions. However, *GNA1* was not identified as a target in the MEWpy optimization. Instead, another gene (commonly signaled for overexpression) involved in the production of chondroitin precursors, *PGM2*, was identified by MEWpy as a potential target for optimization. This gene encodes phosphoglucomutase, showing up in 54 solutions (in the fourth place, Figure 2). As shown in Figure 1, this gene contributes to the production of UDP-glucose precursor.

The second most common modification found was the overexpression of *YAH1*, which encodes yeast adrenodoxin homolog, a ferredoxin involved in heme A biosynthesis by transferring electrons from nicotinamide adenine dinucleotide phosphate reduced form (NADPH) to heme O. The relationship between the overexpression of *YAH1* and the potential improvement of chondroitin production might not be immediately apparent. However, *YAH1* plays a crucial role in the electron transport chain and cellular redox balance within the mitochondria, and its overexpression leads to accumulation of heme A [65]. Consequently, the NAD^+ generated in this process could potentially be utilized in one of the reactions involved in chondroitin production, particularly the reaction catalyzed by UGD. This reaction requires NAD^+ as a co-factor, converting it to NADH during the transformation of UDP-glucose into UDP-glucuronic acid.

The third most frequently identified gene target was the long chain fatty acyl-CoA synthetase gene (*FAA1*), which was observed either as overexpression or underexpression, depending on the proposed solution. Due to the inconsistency in the recommended gene expression for this gene, it can be inferred that its contribution to the enhancement of chondroitin production might not be significant.

Preprints (www.preprints.org) | NOT PEER-REVIEWED | Posted: 20 December 2023 doi:10.20944/preprints202312.1479.v1

The solutions with higher BPCY are described in Table 4. Among the genes identified in the solutions with highest BPCY, only *QRI1* and *PCM1* were found to be directly involved in the pathways associated with chondroitin production (Figure 1).

Table 4. Optimization results obtained for *Saccharomyces cerevisiae* model using MEWpy tool, allowing for a maximum of 10 modifications. Growth rate and chondroitin production rate were predicted by phenotype simulations using parsimonious flux balance analysis (pFBA) and are presented in units of h^{-1} and mmol/g_{DW}/h, respectively. BPCY was calculated by multiplying biomass growth rate by the flux of secreted product, and then dividing by the flux of consumed substrate. WYIELD is the weighted sum of the minimum and maximum product fluxes, with a default weight of 0.3 for maximum and 0.7 for minimum. Flux variability analysis (FVA) results are shown as minimum and maximum chondroitin obtained for fixed biomass.

Solution	BPCY	WYIELD	Genes modified			Predicted phenotype (pFBA)		FVA	
			Knock-out	Under expression	Over expression	Biomass (h^{-1})	Chondroitin flux (mmol/g_{DW}/h)	Minimum chondroitin flux (mmol/g_{DW}/h)	Maximum chondroitin flux (mmol/g_{DW}/h)
1	0.04375	0.60872	*DNF2, CTS1*	*CRD1, LYP1, FAA1*	*YAH1, QRI1, PCM1, CAB5*	0.7317	0.5980	0.5980	0.9358
2	0.04374	0.60872	*FAA1, POT1, CTS1*	*MAL31, ARG8*	*YAH1, PCM1, ALD2*	0.7316	0.5980	0.5980	0.9358
3	0.04335	0.60876	*ENO1, CTS1*	*ERG10*	*FAA1, YAH1, AAT1, POF1, CTA1, PCM1, MAL31*	0.7248	0.5981	0.5981	0.9365

Gene descriptions: *AAT1* - aspartate aminotransferase; *ALD2* - aldehyde dehydrogenase; *ARG8* - acetylornithine aminotransferase; *CAB5* - subunit of the CoA-Synthesizing Protein Complex; *CRD1* - cardiolipin synthase; *CTA1* - catalase A; *CTS1* - endochitinase; *DNF2* – phospholipid-transporting ATPase; *ENO1* - enolase I; *ERG10* - acetyl-CoA C-acetyltransferase; *FAA1* - long chain fatty acyl-CoA synthetase; *LYP1* - lysine permease; *MAL31* - maltose permease; *PCM1* - *N*-acetylglucosamine-phosphate mutase; *POF1* - nicotinamide mononucleotide-specific adenylyltransferase, *POT1* - 3-ketoacyl-CoA thiolase; *QRI1* - UDP-*N*-acetylglucosamine pyrophosphorylase; *YAH1* - yeast adrenodoxin homolog.

However, there are several indirect relationships where modifications to other gene expressions may impact the *in silico* chondroitin production. For instance, the overexpression of the gene *POF1*, which encodes nicotinamide mononucleotide-specific adenylyltransferase, catalyzes the conversion of nicotinamide mononucleotide to nicotinamide adenine dinucleotide (NAD^+), an essential co-factor in chondroitin production, as discussed earlier. Therefore, the identification of *POF1* overexpression may be related with attempting to improve NAD^+ pool. Additionally, *CTS1*, which encodes endochitinase, was identified as a knockout target. As observed Figure 1, chitin formation competes with chondroitin production pathway for UDP-acetylglucosamine substrate. Knocking out *CTS1* could redirect cellular resources and energy that would have been used for chitin breakdown towards the biosynthesis of chondroitin. This redirection could enhance the overall yield and efficiency of chondroitin production.

The size of the resulting solutions was between 8 to 10 gene modifications. However, the BPCY was not higher than the one obtained in the OptFlux solutions, where only one gene expression was altered. In terms of FVA analysis, the robustness from MEWpy solutions was neither higher nor lower than the ones from OptFlux approach. Also, changing the gene expression of 8 to 10 genes would be difficult to implement and would possibly significantly affect the *S. cerevisiae* growth. Therefore, the optimization was again run now limiting the number of modifications to 3. The new optimization

Preprints (www.preprints.org) | NOT PEER-REVIEWED | Posted: 20 December 2023 doi:10.20944/preprints202312.1479.v1

using MEWpy led to 28 solutions. These solutions included modifications in 14 different genes. The frequency and expression value of each gene throughout the solutions is presented in Figure 3.

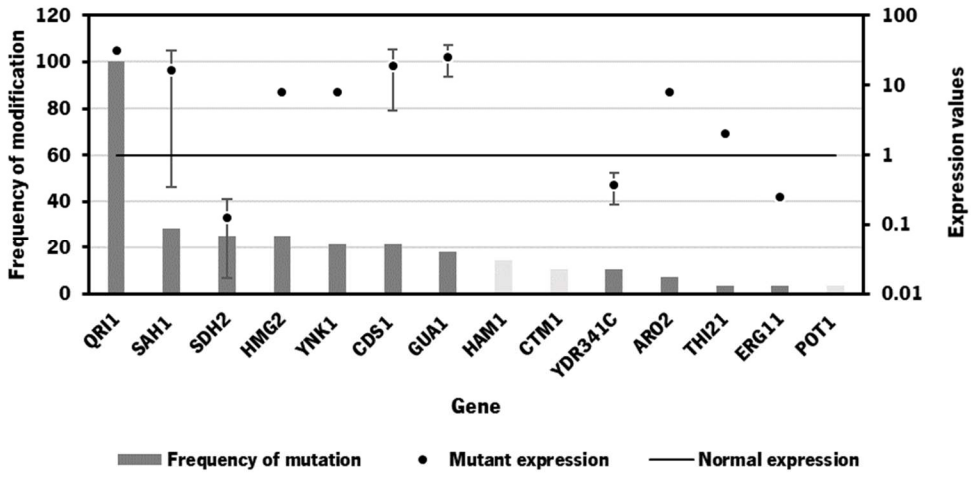

Figure 3. Frequency and expression values of genes in the solutions from optimization of *Saccharomyces cerevisiae* model using MEWpy tool, limiting number of modifications to 3. The mutant expression (in dots) represents the average expression value. Mutant gene expression values higher than 1 represent overexpression, while values of expression lower than 1 represent underexpression. Deletions are represented in light grey bars.

In this case, all solutions included *QRI1* overexpression, which was also predicted in the above-mentioned approaches (Table 3 and Figure 2). The best solutions in terms of BPCY are described in Table 5.

Table 5. Optimization results obtained for *Saccharomyces cerevisiae* model using MEWpy tool, allowing for a maximum of 3 modifications. Growth rate and chondroitin production rate were predicted by phenotype simulations using parsimonious flux balance analysis (pFBA) and are presented in units of h^{-1} and mmol/g_{DW}/h, respectively. BPCY was calculated by multiplying biomass growth rate by the flux of secreted product and then dividing by the flux of consumed substrate. WYIELD is the weighted sum of the minimum and maximum product fluxes, with a default weight of 0.3 for maximum and 0.7 for minimum. Flux variability analysis (FVA) results are shown as minimum and maximum chondroitin obtained for fixed biomass.

Solution	BPCY	WYIELD	Genes modified			Predicted phenotype (pFBA)		FVA	
			Knock-out	Under expression	Over expression	Biomass (h^{-1})	Chondroitin flux (mmol/g_{DW}/h)	Minimum chondroitin flux (mmol/g_{DW}/h)	Maximum chondroitin flux (mmol/g_{DW}/h)
1	0.04375	0.83445	-	-	*QRI1*	0.7317	0.5980	0.5980	0.9358
2	0.01488	2.80306	*CTM1*	*CDS1*	*QRI1*	0.0541	0.6131	0.6131	3.7416
3	0.04359	0.83489	*HAM1*	*SDH2*	*QRI1*	0.7288	0.5980	0.5980	0.9364

Gene descriptions: *CDS1* - phosphatidate cytidylyltransferase; *CTM1* - cytochrome c lysine methyltransferase; *HAM1* - Nucleoside triphosphate pyrophosphohydrolase; *QRI1* – uridine diphosphate-*N*-acetylglucosamine pyrophosphorylase; SDH2 - iron-sulfur protein subunit of succinate dehydrogenase.

 doi:10.20944/preprints202312.1479.v1

As the BPCY values were still low, attempts to find more efficient mutants were made by combining several of the identified promising modifications *in silico* (Table 6). However, the obtained phenotypes of engineered strains with cumulative mutations did not exhibit improved BPCY nor chondroitin production compared to the ones with single modifications.

For future work, other types of models should be explored for more meaningful results on the identification of targets for metabolic engineering. While GEMs can give insights into novel metabolic engineering targets, the phenotype prediction could be more accurate if kinetic data, enzyme usage-constraints and regulatory information were included in the model. For example, GECKO is a method that enhances a GEM to account for enzymes as part of reactions and has been applied to a *S. cerevisiae* model [66].

Table 6. Attempts to obtain higher chondroitin production *in silico* by combining promising gene overexpression targets. Results from simulations in OptFlux using parsimonious flux balance analysis (pFBA) as simulation method for growth rate and chondroitin production rate, are presented in units of h^{-1} and mmol/g_{DW}/h, respectively. BPCY was calculated by multiplying biomass by product and then dividing by substrate consumed, as predicted by pFBA.

Overexpressions	Biomass (h^{-1})	Chondroitin flux (mmol/g_{DW}/h)	BPCY
PCM1, QRI1	0.7317	0.5980	0.04375
PCM1, GNA1	0.7317	0.5980	0.04375
QRI1, GNA1	0.7317	0.5980	0.04375
PCM1, QRI1, GNA1	0.7317	0.5980	0.04375

Gene descriptions: *GNA1* - glucosamine-6-phosphate acetyltransferase; *PCM1* - *N*-acetylglucosamine-phosphate mutase; *QRI1* – uridine diphosphate-*N*-acetylglucosamine pyrophosphorylase

3.2. Flasks fermentations

The reports on the use of eukaryotic microorganisms for chondroitin or chondroitin sulfate production are still very limited. The first study on this area used *P. pastoris* to express the sulfotransferases that were then used to sulfate a chondroitin backbone produced by an engineered *Bacillus subtilis* strain [7]. The same group then engineered a *P. pastoris* strain containing both chondroitin biosynthesis and sulfonation modules, that was able to reach a production of 2.1 g/L chondroitin sulfate with a sulfonation degree of 4.0%. [8]. That work is the only one using a eukaryotic microorganism for chondroitin production. More recently, the same group also engineered a *P. pastoris* strain to produce another complex glycosaminoglycan, namely heparin [67].

To evaluate the ability of a widely used eukaryotic microorganism to potentially host industrial biotechnological process of chondroitin production, we applied efforts to produce chondroitin in *S. cerevisiae*. However, after transforming the plasmids carrying the designed pathways for chondroitin production, the transformants were rare, and after picking colonies from agar plates, some colonies were not able to grow on pre-inoculum liquid medium. Figure 4 shows the performance on chondroitin production by the few transformants we were able to test.

Preprints (www.preprints.org) | NOT PEER-REVIEWED | Posted: 20 December 2023 doi:10.20944/preprints202312.1479.v1

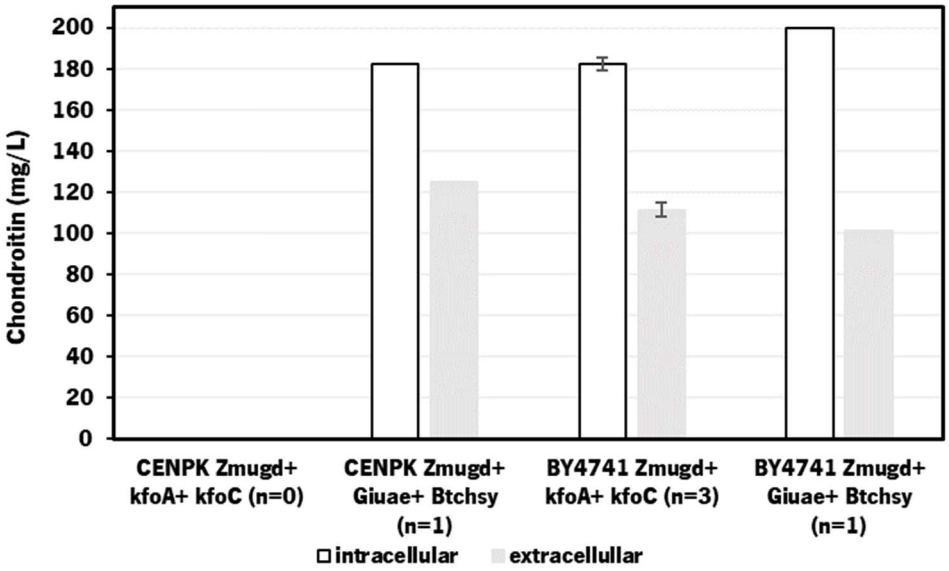

Figure 4. Chondroitin production in engineered *Saccharomyces cerevisiae* CEN.PK2-1C and BY4741 strains.

S. cerevisiae is often used as a host organism for the expression of heterologous genes and can carry multiple plasmids simultaneously. However, introducing multiple plasmids into a yeast cell can have various effects on cell growth and physiology. Some potential problems that may arise include: (a) metabolic burden - the presence of multiple plasmids and the expression of heterologous genes can impose an additional metabolic burden on the host yeast cell, resulting in reduced growth rates and compromised cell viability; (b) competitive replication - plasmids often compete for limited cellular resources during replication, leading to instability and loss of one or both plasmids over time, leading to a heterogeneous population of cells with varying plasmid content; and (c) induced stress responses - the expression of foreign genes may induce stress responses in the host cell, triggering various regulatory mechanisms that can affect cellular homeostasis and growth.

To overcome these potential issues, several strategies can be employed including: (a) balanced expression of genes - fine-tuning the expression levels of multiple genes can help alleviate the metabolic burden and minimize adverse effects on cell growth and physiology; (b) strain engineering - using engineered yeast strains with improved capabilities for handling metabolic stress or expressing foreign genes can help mitigate the negative impacts on cell growth; and (c) adaptative laboratory evolution - improving the performance of microbial strains under specific conditions by subjecting a population of microorganisms to prolonged periods of growth under controlled selective pressure, allows the natural selection of beneficial mutations that may result in yeast strains adapted to efficiently manage the additional genetic load. The combination of these strategies might result in robust yeast strains capable of efficiently carrying multiple plasmids and expressing heterologous genes without compromising growth or productivity.

Despite few viable colonies were obtained in transformations, the strains herein constructed were able to produce chondroitin between 182 and 200 mg/L, without significant differences between the different constructs and strains.

Comparing to the other work describing chondroitin production using *P.* pastoris [67], the genes used for the chondroitin production module were *kfoC*, *kfoA* (from *E. coli* K4), and *tuaD* (UDP-glucose dehydrogenase from *B. subtilis*) which yielded only 5.5 mg/L chondroitin. After further codon-optimized of the genes, and changing the bioprocess to a fed-batch fermentation, the chondroitin production increased to 2.1 g/L. This suggests that the chondroitin production herein obtained can also be further improved using some of the strategies discussed above.

Furthermore, since the robustness of the engineered strains, culture medium and operational mode need additional optimizations, further genetic modifications on the host harboring the

 doi:10.20944/preprints202312.1479.v1

heterologous pathway were not performed. Once a robust host strain is constructed, further modifications, such as *QRI1, GNA1 or PCM1* overexpression, as suggested by the bioinformatic approaches herein described, should be performed.

4. Conclusions

Chondroitin sulfate stands as a valuable natural compound, with its distinct sulfation patterns and properties leading to a wide range of practical uses. Its biotechnological production presents an intriguing opportunity. As *S. cerevisiae* is a robust, fast-growing, and easily mutated host, it has been selected to be engineered with chondroitin biosynthetic pathways. Also, this is an alternative host that should be considered for chondroitin production due to its ability to perform post-translational modifications. Since the application of computational-aided metabolic engineering might help discover critical bottlenecks in its heterologous biosynthesis, a metabolic model and flux analysis has been herein used for strain design. The model yeastGEM_c has been constructed using yeast GEM as scaffold in which chondroitin production reactions and genes have been included. Using evolutionary algorithms, several promising novel targets, such as *QRI1, GNA1* or *PCM1* overexpression, have been identified as promising to improve chondroitin titers of engineered *S. cerevisiae* strains. Thus, the strategy reported here should be useful in developing industrial *S. cerevisiae* strains capable of efficient chondroitin production. Furthermore, novel biosynthetic pathways have been evaluated for producing chondroitin in this host, and 125 mg/L of extracellular chondroitin have been obtained through flask fermentation. The use of these pathways to construct the predicted engineered strains, in combination with other methods, such as integration of genes in yeast genome and adaptative lab evolution, can lead to further improved chondroitin yields.

Supplementary Materials: The following supporting information can be downloaded at: Preprints.org, Table S1: Primers used in this study; Table S2. Codon-optimized gene sequences (5' → 3') for *Saccharomyces cerevisiae*.

Author Contributions: M.R.C. performed the experiments, analyzed the data and drafted the manuscript. O.D. conducted MEWpy experiments on Python. J.L.R. and L.R.R. supervised and coordinated the study and provided feedback and suggestions on the manuscript. L.R.R. provided funds for the research development. All authors read and agreed to the published version of the manuscript.

Funding: This study was supported by the Portuguese Foundation for Science and Technology (FCT) under the scope of the strategic funding of UIDB/04469/2020 unit. The authors acknowledge FCT for funding MRC doctoral grant SFRH/BD/132998/2017 and further extension COVID/BD/152454/2022.

Conflicts of Interest: The authors declare no conflict of interest. The funders had no role in the design of the study; in the collection, analyses, or interpretation of data; in the writing of the manuscript; or in the decision to publish the results.

References

1. Couto, M.R.; Rodrigues, J.L.; Rodrigues, L.R. Heterologous production of chondroitin. *Biotechnol. Reports* **2022**, *33*, e00710, doi:10.1016/j.btre.2022.e00710.
2. Cress, B.F.; Englaender, J.A.; He, W.; Kasper, D.; Linhardt, R.J.; Koffas, M.A.G. Masquerading microbial pathogens: Capsular polysaccharides mimic host-tissue molecules. *FEMS Microbiol. Rev.* **2014**, *38*, 660–697, doi:10.1111/1574-6976.12056.
3. Cimini, D.; Carlino, E.; Giovane, A.; Argenzio, O.; Dello Iacono, I.; De Rosa, M.; Schiraldi, C. Engineering a branch of the UDP-precursor biosynthesis pathway enhances the production of capsular polysaccharide in *Escherichia coli* O5:K4:H4. *Biotechnol. J.* **2015**, *10*, 1307–1315, doi:10.1002/biot.201400602.
4. Jin, P.; Zhang, L.; Yuan, P.; Kang, Z.; Du, G.; Chen, J. Efficient biosynthesis of polysaccharides chondroitin and heparosan by metabolically engineered *Bacillus subtilis*. *Carbohydr. Polym.* **2016**, *140*, 424–432, doi:10.1016/j.carbpol.2015.12.065.
5. He, W.; Fu, L.; Li, G.; Andrew Jones, J.; Linhardt, R.J.; Koffas, M.; Jones, J.A.; Linhardt, R.J.; Koffas, M.; Andrew Jones, J.; et al. Production of chondroitin in metabolically engineered *E. coli*. *Metab. Eng.* **2015**, *27*, 92–100, doi:10.1016/j.ymben.2014.11.003.
6. Cheng, F.; Luozhong, S.; Yu, H.; Guo, Z. Biosynthesis of chondroitin in engineered *Corynebacterium glutamicum*. *J. Microbiol. Biotechnol.* **2019**, *29*, 392–400, doi:10.4014/JMB.1810.10062.

7. Zhou, Z.; Li, Q.; Huang, H.; Wang, H.; Wang, Y.; Du, G.; Chen, J.; Kang, Z. A microbial–enzymatic strategy for producing chondroitin sulfate glycosaminoglycans. *Biotechnol. Bioeng.* **2018**, *115*, 1561–1570, doi:10.1002/bit.26577.
8. Jin, X.; Zhang, W.; Wang, Y.; Sheng, J.; Xu, R.; Li, J.; Du, G.; Kang, Z. Biosynthesis of non-animal chondroitin sulfate from methanol using genetically engineered *Pichia pastoris*. *Green Chem.* **2021**, *23*, 4365–4374, doi:10.1039/d1gc00260k.
9. Desko, M.M.; Gross, D.A.; Kohler, J.J. Effects of N-glycosylation on the activity and localization of GlcNAc-6-sulfotransferase 1. *Glycobiology* **2009**, *19*, 1068–1077, doi:10.1093/glycob/cwp092.
10. Badri, A.; Williams, A.; Awofiranye, A.; Datta, P.; Xia, K.; He, W.; Fraser, K.; Dordick, J.S.; Linhardt, R.J.; Koffas, M.A.G.G. Complete biosynthesis of a sulfated chondroitin in *Escherichia coli*. *Nat. Commun.* **2021**, *12*, 1–10, doi:10.1038/s41467-021-21692-5.
11. Nielsen, J. Yeast Systems Biology: Model Organism and Cell Factory. *Biotechnol. J.* **2019**, *14*, 1–9, doi:10.1002/biot.201800421.
12. Li, M.; Borodina, I. Application of synthetic biology for production of chemicals in yeast *Saccharomyces cerevisiae*. *FEMS Yeast Res.* **2015**, *15*, 1–12, doi:10.1111/1567-1364.12213.
13. Gupta, S.K.; Shukla, P. Sophisticated cloning, fermentation, and purification technologies for an enhanced therapeutic protein production: A review. *Front. Pharmacol.* **2017**, *8*, 1–17, doi:10.3389/fphar.2017.00419.
14. Lopes, H.; Rocha, I. Genome-scale modeling of yeast: chronology, applications and critical perspectives. *FEMS Yeast Res.* **2017**, *17*, 1–14, doi:10.1093/femsyr/fox050.
15. Vieira, V.; Maia, P.; Rocha, M.; Rocha, I. Comparison of pathway analysis and constraint-based methods for cell factory design. *BMC Bioinformatics* **2019**, *20*, 1–15, doi:10.1186/s12859-019-2934-y.
16. Maia, P.; Rocha, M.; Rocha, I. *In silico* constraint-based strain optimization methods: the quest for optimal cell factories. *Microbiol. Mol. Biol. Rev.* **2016**, *80*, 45–67, doi:10.1128/mmbr.00014-15.
17. Bi, X.; Liu, Y.; Li, J.; Du, G.; Lv, X.; Liu, L. Construction of multiscale genome-scale metabolic models: frameworks and challenges. *Biomolecules* **2022**, *12*, 1–21, doi:10.3390/biom12050721.
18. Ng, R.H.; Lee, J.W.; Baloni, P.; Diener, C.; Heath, J.R.; Su, Y. Constraint-based reconstruction and analyses of metabolic models: open-source Python tools and applications to cancer. *Front. Oncol.* **2022**, *12*, 1–23, doi:10.3389/fonc.2022.914594.
19. Mardinoglu, A.; Nielsen, J. Systems medicine and metabolic modelling. *J. Intern. Med.* **2012**, *271*, 142–154, doi:10.1111/j.1365-2796.2011.02493.x.
20. Zhang, C.; Hua, Q. Applications of genome-scale metabolic models in biotechnology and systems medicine. *Front. Physiol.* **2016**, *6*, 1–8, doi:10.3389/fphys.2015.00413.
21. Fang, X.; Lloyd, C.J.; Palsson, B.O. Reconstructing organisms *in silico*: genome-scale models and their emerging applications. *Nat. Rev. Microbiol.* **2020**, *18*, 731–743, doi:10.1038/s41579-020-00440-4.
22. Gu, C.; Kim, G.B.; Kim, W.J.; Kim, H.U.; Lee, S.Y. Current status and applications of genome-scale metabolic models. *Genome Biol.* **2019**, *20*, 1–18, doi:10.1186/s13059-019-1730-3.
23. Chen, X.; Xu, G.; Xu, N.; Zou, W.; Zhu, P.; Liu, L.; Chen, J. Metabolic engineering of *Torulopsis glabrata* for malate production. *Metab. Eng.* **2013**, *19*, 10–16, doi:10.1016/j.ymben.2013.05.002.
24. Xu, G.; Zou, W.; Chen, X.; Xu, N.; Liu, L.; Chen, J. Fumaric acid production in *Saccharomyces cerevisiae* by *in silico a*ided metabolic engineering. *PLoS One* **2012**, *7*, 1–10, doi:10.1371/journal.pone.0052086.
25. Otero, J.M.; Cimini, D.; Patil, K.R.; Poulsen, S.G.; Olsson, L.; Nielsen, J. Industrial systems biology of *Saccharomyces cerevisiae* enables novel succinic acid cell factory. *PLoS One* **2013**, *8*, 1–10, doi:10.1371/journal.pone.0054144.
26. Song, C.W.; Kim, D.I.; Choi, S.; Jang, J.W.; Lee, S.Y. Metabolic engineering of *Escherichia coli* for the production of fumaric acid. *Biotechnol. Bioeng.* **2013**, *110*, 2025–2034, doi:10.1002/bit.24868.
27. Chen, X.; Wu, J.; Song, W.; Zhang, L.; Wang, H.; Liu, L. Fumaric acid production by *Torulopsis glabrata*: Engineering the urea cycle and the purine nucleotide cycle. *Biotechnol. Bioeng.* **2015**, *112*, 156–167, doi:10.1002/bit.25334.
28. Harder, B.J.; Bettenbrock, K.; Klamt, S. Model-based metabolic engineering enables high yield itaconic acid production by *Escherichia coli*. *Metab. Eng.* **2016**, *38*, 29–37, doi:10.1016/j.ymben.2016.05.008.
29. Mishra, P.; Lee, N.-R.; Lakshmanan, M.; Kim, M.; Kim, B.-G.; Lee, D.-Y. Genome-scale model-driven strain design for dicarboxylic acid production in *Yarrowia lipolytica*. *BMC Syst. Biol.* **2018**, *12*, 12, doi:10.1186/s12918-018-0542-5.
30. Bro, C.; Regenberg, B.; Förster, J.; Nielsen, J. *In silico* aided metabolic engineering of *Saccharomyces cerevisiae* for improved bioethanol production. *Metab. Eng.* **2006**, *8*, 102–111, doi:10.1016/j.ymben.2005.09.007.
31. Yim, H.; Haselbeck, R.; Niu, W.; Pujol-Baxley, C.; Burgard, A.; Boldt, J.; Khandurina, J.; Trawick, J.D.; Osterhout, R.E.; Stephen, R.; et al. Metabolic engineering of *Escherichia coli* for direct production of 1,4-butanediol. *Nat. Chem. Biol.* **2011**, *7*, 445–452, doi:10.1038/nchembio.580.
32. Ng, C.; Jung, M.; Lee, J.; Oh, M.-K. Production of 2,3-butanediol in *Saccharomyces cerevisiae* by *in silico* aided metabolic engineering. *Microb. Cell Fact.* **2012**, *11*, 68, doi:10.1186/1475-2859-11-68.

33. Becker, J.; Zelder, O.; Häfner, S.; Schröder, H.; Wittmann, C. From zero to hero-Design-based systems metabolic engineering of *Corynebacterium glutamicum* for l-lysine production. *Metab. Eng.* **2011**, *13*, 159–168, doi:10.1016/j.ymben.2011.01.003.
34. Park, J.H.; Kim, T.Y.; Lee, K.H.; Lee, S.Y. Fed-batch culture of *Escherichia coli* for L-valine production based on *in silico* flux response analysis. *Biotechnol. Bioeng.* **2011**, *108*, 934–946, doi:10.1002/bit.22995.
35. van Ooyen, J.; Noack, S.; Bott, M.; Reth, A.; Eggeling, L. Improved L-lysine production with *Corynebacterium glutamicum* and systemic insight into citrate synthase flux and activity. *Biotechnol. Bioeng.* **2012**, *109*, 2070–2081, doi:10.1002/bit.24486.
36. Jung, Y.K.; Kim, T.Y.; Park, S.J.; Lee, S.Y. Metabolic engineering of *Escherichia coli* for the production of polylactic acid and its copolymers. *Biotechnol. Bioeng.* **2010**, *105*, 161–171, doi:10.1002/bit.22548.
37. Poblete-Castro, I.; Binger, D.; Rodrigues, A.; Becker, J.; Martins Dos Santos, V.A.P.; Wittmann, C. In-silico-driven metabolic engineering of *Pseudomonas putida* for enhanced production of poly-hydroxyalkanoates. *Metab. Eng.* **2013**, *15*, 113–123, doi:10.1016/j.ymben.2012.10.004.
38. Kildegaard, K.R.; Jensen, N.B.; Schneider, K.; Czarnotta, E.; Özdemir, E.; Klein, T.; Maury, J.; Ebert, B.E.; Christensen, H.B.; Chen, Y.; et al. Engineering and systems-level analysis of *Saccharomyces cerevisiae* for production of 3-hydroxypropionic acid via malonyl-CoA reductase-dependent pathway. *Microb. Cell Fact.* **2016**, *15*, 1–13, doi:10.1186/s12934-016-0451-5.
39. Yang, J.E.; Park, S.J.; Kim, W.J.; Kim, H.J.; Kim, B.J.; Lee, H.; Shin, J.; Lee, S.Y. One-step fermentative production of aromatic polyesters from glucose by metabolically engineered *Escherichia coli* strains. *Nat. Commun.* **2018**, *9*, 79, doi:10.1038/s41467-017-02498-w.
40. Kim, M.; Sang Yi, J.; Kim, J.; Kim, J.N.; Kim, M.W.; Kim, B.G. Reconstruction of a high-quality metabolic model enables the identification of gene overexpression targets for enhanced antibiotic production in *Streptomyces coelicolor* A3(2). *Biotechnol. J.* **2014**, *9*, 1185–1194, doi:10.1002/biot.201300539.
41. Huang, D.; Wen, J.; Wang, G.; Yu, G.; Jia, X.; Chen, Y. *In silico* aided metabolic engineering of *Streptomyces roseosporus* for daptomycin yield improvement. *Appl. Microbiol. Biotechnol.* **2012**, *94*, 637–649, doi:10.1007/s00253-011-3773-6.
42. Chemler, J.A.; Fowler, Z.L.; McHugh, K.P.; Koffas, M.A.G. Improving NADPH availability for natural product biosynthesis in *Escherichia coli* by metabolic engineering. *Metab. Eng.* **2010**, *12*, 96–104, doi:10.1016/j.ymben.2009.07.003.
43. Bhan, N.; Xu, P.; Khalidi, O.; Koffas, M.A.G. Redirecting carbon flux into malonyl-CoA to improve resveratrol titers: Proof of concept for genetic interventions predicted by OptForce computational framework. *Chem. Eng. Sci.* **2013**, *103*, 109–114, doi:10.1016/j.ces.2012.10.009.
44. Xu, P.; Ranganathan, S.; Fowler, Z.L.; Maranas, C.D.; Koffas, M.A.G.G. Genome-scale metabolic network modeling results in minimal interventions that cooperatively force carbon flux towards malonyl-CoA. *Metab. Eng.* **2011**, *13*, 578–587, doi:10.1016/j.ymben.2011.06.008.
45. Lu, H.; Li, F.; Sánchez, B.J.; Zhu, Z.; Li, G.; Domenzain, I.; Marcišauskas, S.; Anton, P.M.; Lappa, D.; Lieven, C.; et al. A consensus *S. cerevisiae* metabolic model Yeast8 and its ecosystem for comprehensively probing cellular metabolism. *Nat. Commun.* **2019**, *10*, doi:10.1038/s41467-019-11581-3.
46. Rocha, I.; Maia, P.; Evangelista, P.; Vilaça, P.; Soares, S.; Pinto, J.P.; Nielsen, J.; Patil, K.R.; Ferreira, E.C.; Rocha, M. OptFlux: an open-source software platform for *in silico* metabolic engineering. *BMC Syst. Biol.* **2010**, *4*, 1–12, doi:10.1186/1752-0509-4-45.
47. Lewis, N.E.; Hixson, K.K.; Conrad, T.M.; Lerman, J.A.; Charusanti, P.; Polpitiya, A.D.; Adkins, J.N.; Schramm, G.; Purvine, S.O.; Lopez-Ferrer, D.; et al. Omic data from evolved *E. coli* are consistent with computed optimal growth from genome-scale models. *Mol. Syst. Biol.* **2010**, *6*, 1–13, doi:10.1038/msb.2010.47.
48. Zitzler, E.; Laumanns, M.; Thiele, L. SPEA2: Improving the Strength Pareto Evolutionary Algorithm. *Evol. Methods Des. Optim. Control with Appl. to Ind. Probl.* **2001**, 95–100, doi:10.3929/ethz-a-004284029.
49. Pereira, V.; Cruz, F.; Rocha, M. MEWpy: a computational strain optimization workbench in Python. *Bioinformatics* **2021**, 1–3, doi:10.1093/bioinformatics/btab013.
50. Deb, K.; Pratap, A.; Agarwal, S.; Meyarivan, T. A fast and elitist multiobjective genetic algorithm: NSGA-II. *IEEE Trans. Evol. Comput.* **2002**, *6*, 182–197, doi:10.1109/4235.996017.
51. Mahadevan, R.; Schilling, C.H. The effects of alternate optimal solutions in constraint-based genome-scale metabolic models. *Metab. Eng.* **2003**, *5*, 264–276, doi:10.1016/j.ymben.2003.09.002.
52. Entian, K.-D.; Kötter, P. 25 Yeast genetic strain and plasmid collections. In *Methods in Microbiology*; Stansfield, I., Stark, M.J.R., Eds.; Elsevier, 2007; Vol. 36, pp. 629–666 ISBN 0123694787.
53. Brachmann, C.B.; Davies, A.; Cost, G.J.; Caputo, E.; Li, J.; Hieter, P.; Boeke, J.D. Designer deletion strains derived from *Saccharomyces cerevisiae* S288C: A useful set of strains and plasmids for PCR-mediated gene disruption and other applications. *Yeast* **1998**, *14*, 115–132, doi:10.1002/(SICI)1097-0061(19980130)14:2<115::AID-YEA204>3.0.CO;2-2.

54. Chen, Y.; Partow, S.; Scalcinati, G.; Siewers, V.; Nielsen, J. Enhancing the copy number of episomal plasmids in *Saccharomyces cerevisiae* for improved protein production. *FEMS Yeast Res.* **2012**, *12*, 598–607, doi:10.1111/j.1567-1364.2012.00809.x.
55. Couto, M.R.; Rodrigues, J.L.; Rodrigues, L.R. Cloning, expression and characterization of UDP-glucose dehydrogenases. *Life* **2021**, *11*, 1201, doi:10.3390/life11111201.
56. Gietz, R.D.; Woods, R.A. Transformation of yeast by lithium acetate/single-stranded carrier DNA/polyethylene glycol method. In *Methods in Enzymology*; 2002; Vol. 350, pp. 87–96.
57. Bitter, T.; Muir, H.M. A modified uronic acid carbazole reaction. *Anal. Biochem.* **1962**, *4*, 330–334, doi:10.1016/0003-2697(62)90095-7.
58. Shaw, J.A.; Mol, P.C.; Bowers, B.; Silverman, S.J.; Valdivieso, M.H.; Duran, A.; Cabib, E. The function of chitin synthases 2 and 3 in the *Saccharomyces cerevisiae* cell cycle. *J. Cell Biol.* **1991**, *114*, 111–123, doi:10.1083/jcb.114.1.111.
59. Lesage, G.; Bussey, H. Cell Wall Assembly in *Saccharomyces cerevisiae* . *Microbiol. Mol. Biol. Rev.* **2006**, *70*, 317–343, doi:10.1128/mmbr.00038-05.
60. Orlean, P. Architecture and biosynthesis of the *Saccharomyces cerevisiae* cell wall. *Genetics* **2012**, *192*, 775–818, doi:10.1534/genetics.112.144485.
61. Klis, F.M.; Mol, P.; Hellingwerf, K.; Brul, S. Dynamics of cell wall structure in *Saccharomyces cerevisiae*. *FEMS Microbiol. Rev.* **2002**, *26*, 239–256, doi:10.1016/S0168-6445(02)00087-6.
62. Zhang, Q.; Yao, R.; Chen, X.; Liu, L.; Xu, S.; Chen, J.; Wu, J. Enhancing fructosylated chondroitin production in *Escherichia coli* K4 by balancing the UDP-precursors. *Metab. Eng.* **2018**, *47*, 314–322, doi:10.1016/j.ymben.2018.04.006.
63. Wu, J.; Zhang, Q.; Liu, L.; Chen, X.; Liu, J.; Luo, Q. Recombinant *Escherichia coli* for high efficiency production of fructosylated chondroitin and method for making thereof 2019.
64. D'ambrosio, S.; Alfano, A.; Cassese, E.; Restaino, O.F.; Barbuto Ferraiuolo, S.; Finamore, R.; Cammarota, M.; Schiraldi, C.; Cimini, D. Production and purification of higher molecular weight chondroitin by metabolically engineered *Escherichia coli* K4 strains. *Sci. Rep.* **2020**, *10*, 1–10, doi:10.1038/s41598-020-70027-9.
65. Barros, M.H.; Tzagoloff, A. Regulation of the heme A biosynthetic pathway in *Saccharomyces cerevisiae*. *FEBS Lett.* **2002**, *516*, 119–123, doi:10.1016/S0014-5793(02)02514-0.
66. Sánchez, B.J.; Zhang, C.; Nilsson, A.; Lahtvee, P.; Kerkhoven, E.J.; Nielsen, J. Improving the phenotype predictions of a yeast genome-scale metabolic model by incorporating enzymatic constraints. *Mol. Syst. Biol.* **2017**, *13*, 935, doi:10.15252/msb.20167411.
67. Zhang, Y.; Wang, Y.; Zhou, Z.; Wang, P.; Xi, X.; Hu, S.; Xu, R.R.; Du, G.; Li, J.; Chen, J.; et al. Synthesis of bioengineered heparin by recombinant yeast *Pichia pastoris*. *Green Chem.* **2022**, 3180–3192, doi:10.1039/d1gc04672a.